

# **Supplementary Materials for**

## **Spectral Response Analysis: An Indirect and Non-Destructive Methodology for Biocrusts Chlorophyll Quantification**

José Raúl Román, Emilio Rodríguez-Caballero, Borja Rodríguez-Lozano, Beatriz Roncero-Ramos, Sonia Chamizo, Pilar Águila-Carricondo and Yolanda Cantón

**Table S1.** Soil texture, pH, electrical conductivity, total organic carbon (TOC) and total nitrogen (TN) of the three soils employed in this study: Las Amoladeras, El Cautivo and Gádor quarry (from Román et al., 2018).

| Soil types     | Soil texture |              |              | pH          | Electrical Conductivity (mS/cm) | TOC (g/Kg)   | TN (g/Kg)   |
|----------------|--------------|--------------|--------------|-------------|---------------------------------|--------------|-------------|
|                | Sand (%)     | Silt (%)     | Clay (%)     |             |                                 |              |             |
| Las Amoladeras | 61.50 ± 5.10 | 28.40 ± 4.20 | 10.10 ± 2.10 | 8.03 ± 0.04 | 0.16 ± 0.01                     | 21.41 ± 0.96 | 2.07 ± 0.11 |
| El Cautivo     | 29.20 ± 5.40 | 58.60 ± 5.80 | 12.20 ± 4.20 | 8.28 ± 0.12 | 0.13 ± 0.01                     | 3.87 ± 0.09  | 0.57 ± 0.04 |
| Gádor quarry   | 31.20 ± 4.65 | 43.10 ± 2.34 | 25.70 ± 2.80 | 8.57 ± 0.03 | 1.98 ± 0.18                     | 0.24 ± 0.21  | 0.17 ± 0.09 |

2           **Table S2.** Summary of the different spectral indices used in this study. R: reflectance; Q: the first  
 3           derivative of reflectance; RBLUE: reflectance in the blue region, RGREEN: reflectance in the  
 4           green region, RNIR: reflectance in the near-infrared region.

| <b>Index</b>   | <b>Formulation</b>                        | <b>Reference</b>              |
|--|---|-------------------------------|
| <i>Simple ratio or modified simple ratio of reflectance or derivatives</i> |   |                               |
| YCAR   | $R_{600}/R_{680}$                         | Schlemmer et al. (2005)       |
| OCAR   | $R_{630}/R_{680}$                         | Schlemmer et al. (2005)       |
| Vogelman3  | $R_{740}/R_{720}$                         | Vogelman et al. (1993)        |
| SRPI (Simple Ratio Pigment Index)  | $R_{430}/R_{680}$                         | Peñuelas et al. (1994)        |
| Vogelman1  | $Q_{715}/Q_{705}$                         | Vogelman et al. (1993)        |
| dSR1*  | $Q_{725}/Q_{702}$                         | Kochubey and Kazantsev (2007) |
| dSR2*  | $Q_{705}/Q_{722}$                         | Zarco-Tejada et al. (2002)    |
| Datt-CabCx+c   | $R_{860}/(R_{550} * R_{708})$             | Datt (1998)                   |
| PSRI   | $(R_{680} - R_{500})/R_{750}$             | Merzlyak et al. (1999)        |
| mSR705   | $(R_{750} - R_{445})/(R_{705} - R_{445})$ | Sims and Gamon (2002)         |
| BmSR   | $(Q_{722} - Q_{502})/(Q_{700} - Q_{502})$ | le Maire et al. (2004)        |

## 5 Table S2 (Continuation)

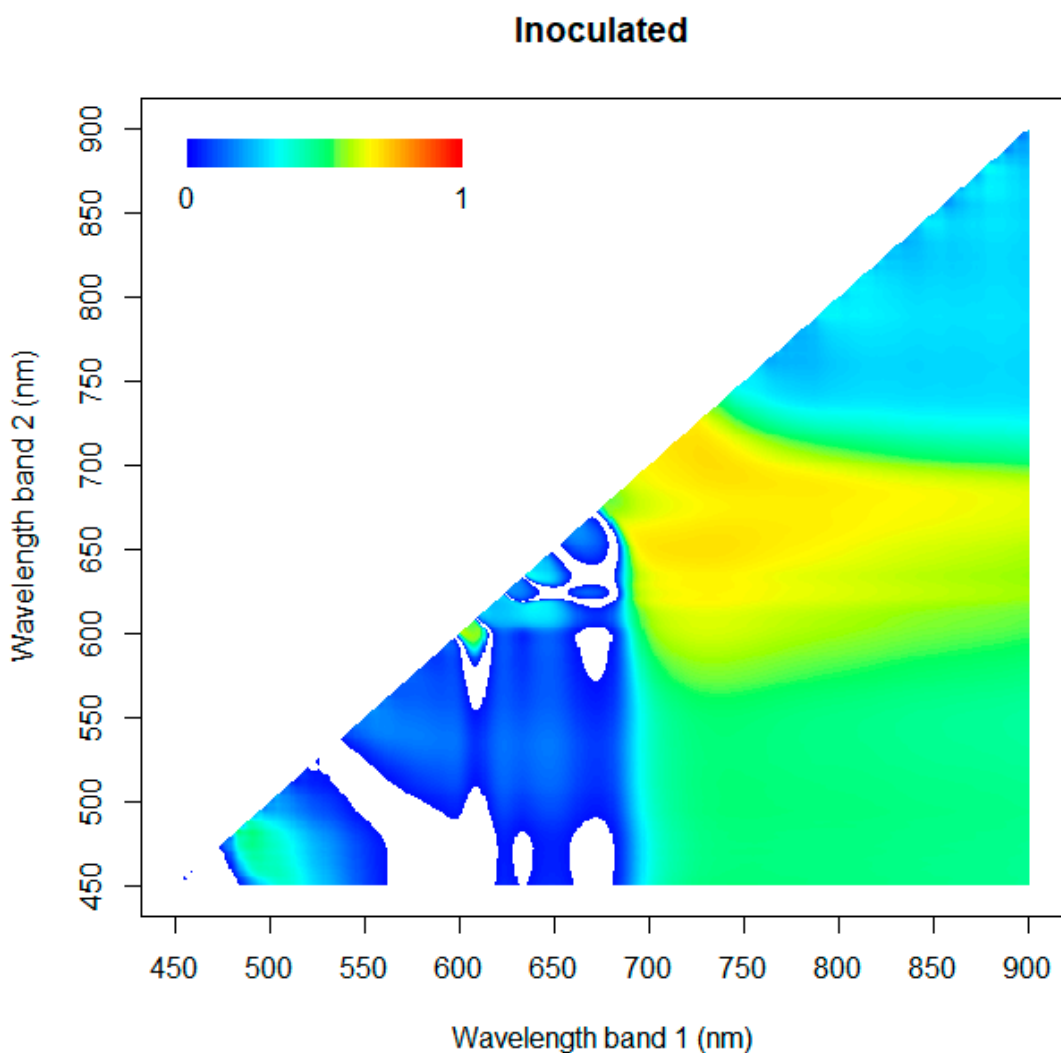
| Index  | Formulation   | Reference                   |
|--|---|-----------------------------|
| <i>Normalized difference of derivatives</i>  |   |                             |
| BND  | $(Q_{722} - Q_{700})/(Q_{722} + Q_{700})$                           | le Maire et al. (2004)      |
| <i>Modified normalized difference of derivatives</i>   |   |                             |
| BmND   | $(Q_{722} - Q_{700})/(Q_{722} + Q_{700} - 2Q_{502})$                | le Maire et al. (2004)      |
| <i>Indices related with red edge derived with derivatives</i>  |   |                             |
| dRE  | First derivative maxima in red-edge region (680-780 nm)             | Filella and Peñuelas (1994) |
| $\Sigma dRE$   | Sum of first derivative reflectance in red-edge region (680-780 nm) | Filella and Peñuelas (1994) |
| EGFR (Ratio of first derivative maxima in red-edge region and green region (530-570 nm))                         | $dRE/dG$  | Penuelas et al. (1994)      |
| EGFN   | $(dRE - dG)/(dRE + dG)$   | Penuelas et al. (1994)      |
| EBAR (Ratio of Sum of first derivative reflectance in red-edge region (680-780 nm) and blue region (490-530 nm)) | $\Sigma dRE/\Sigma dB$  | Xue et al. (2009)           |
| EBAN   | $(\Sigma dRE - \Sigma dB)/(\Sigma dRE + \Sigma dB)$                 | Xue et al. (2009)           |
| EBFR   | $dRE/dB$  | Xue et al. (2009)           |
| EBFN   | $(dRE - dB)/(dRE + dB)$   | Xue et al. (2009)           |

6 Table S2 (Continuation)

| Index  | Formulation  | Reference              |
|--|--|------------------------|
| <i>Broad band indices</i>                                    |  |                        |
| Normalized Difference Vegetation Index(NDVI)                 | $(R_{NIR} - R_{RED}) / (R_{NIR} + R_{RED})$                              | Rouse et al. (1973)    |
| Enhanced Vegetation Index (EVI)                              | $2.5 * (R_{NIR} - R_{RED}) / (R_{NIR} + 6R_{RED} - 7.5R_{BLUE} + 1)$     | Huete et al. (2002)    |
| Soil-adjusted vegetation index (SAVI)                        | $(R_{NIR} - R_{RED}) / (R_{NIR} + R_{RED} + 0.5) * (1 + 0.5)$            | Huete (1988)           |
| Optimized soil-adjusted vegetation index (OSAVI)             | $(R_{NIR} - R_{RED}) / (R_{NIR} + R_{RED} + 0.16) * (1 + 0.16)$          | Rondeaux et al. (1996) |
| Modified Chlorophyll Absorption in Reflectance Index (MCARI) | $[(R_{NIR} - R_{RED}) - 0.2(R_{NIR} + R_{GREEN})] * (R_{NIR} / R_{RED})$ | Daughtry et al. (2000) |
| MCARI/OSAVI  | MCARI/OSAVI  | Daughtry et al. (2000) |
| Simple Ratio Index (SR)                                      | $(R_{NIR} / R_{RED})$  | Jordan (1969)          |
| Modified Simple Ratio Index (MSR)                            | $[(R_{NIR} / R_{RED}) - 1] / [(R_{NIR} / R_{RED}) - 1]^{1/2}$            | Chen (1996)            |
| Crust Index (CI)   | $1 - (R_{RED} - R_{BLUE}) / (R_{RED} - R_{BLUE})$                        | Karnieli, 1997         |
| Biological Soil Crust Index (BSCI)                           | $\frac{1 - 2 \times  R_{RED} - R_{GREEN} }{R_{GRNIR}^{mean}}$            | Chen et al. (2005)     |

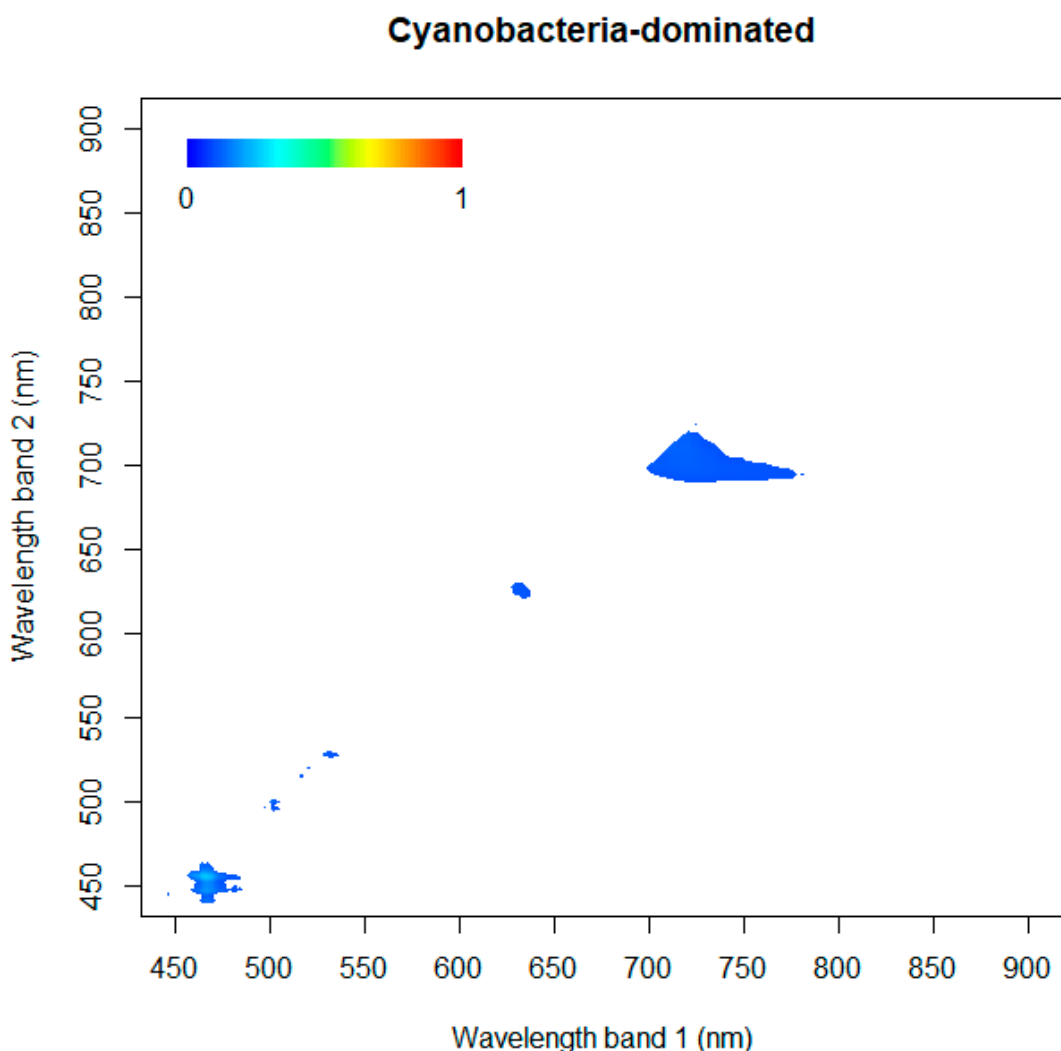
7 Table S2 (Continuation)

| Index  | Formulation  | Reference                            |
|--|--|--------------------------------------|
| <i>Others</i>  |  |                                      |
| MCARI <sub>[705,750]</sub>   | $\frac{[(R_{750} - R_{705}) - 0.2(R_{750} - R_{550})]}{(R_{750}/R_{705})}$ | Wu et al. (2008)                     |
| Blog 1/R737  | the first derivative of logarithm<br>$1/R_{737}$                           | Yoder and Pettigrew-Crosby<br>(1995) |
| DD   | $(R_{749} - R_{720})/(R_{701} - R_{672})$                                  | le Maire et al. (2004)               |
| SIPI (Structure Insensitive<br>Pigment Index)                              | $(R_{800} - R_{445})/(R_{800} - R_{680})$                                  | Peñuelas et al. (1995)               |
| Vogelman2  | $(R_{734} - R_{747})/(R_{715} + 726)$                                      | Vogelman et al. (1993)               |
| PRI (Photochemical reflectance<br>index) * Ci (chlorophyll ratio<br>index) | $[(R_{570} - R_{530})/(R_{570} + R_{530})]^*$<br>$[(R_{760}/R_{700}) - 1]$ | Garrity et al., (2011)               |
| DFDS_ICCW  | sum of $Q_{675-680}$ - sum of $Q_{640-674}$                                | Zhang et al. (2014)                  |



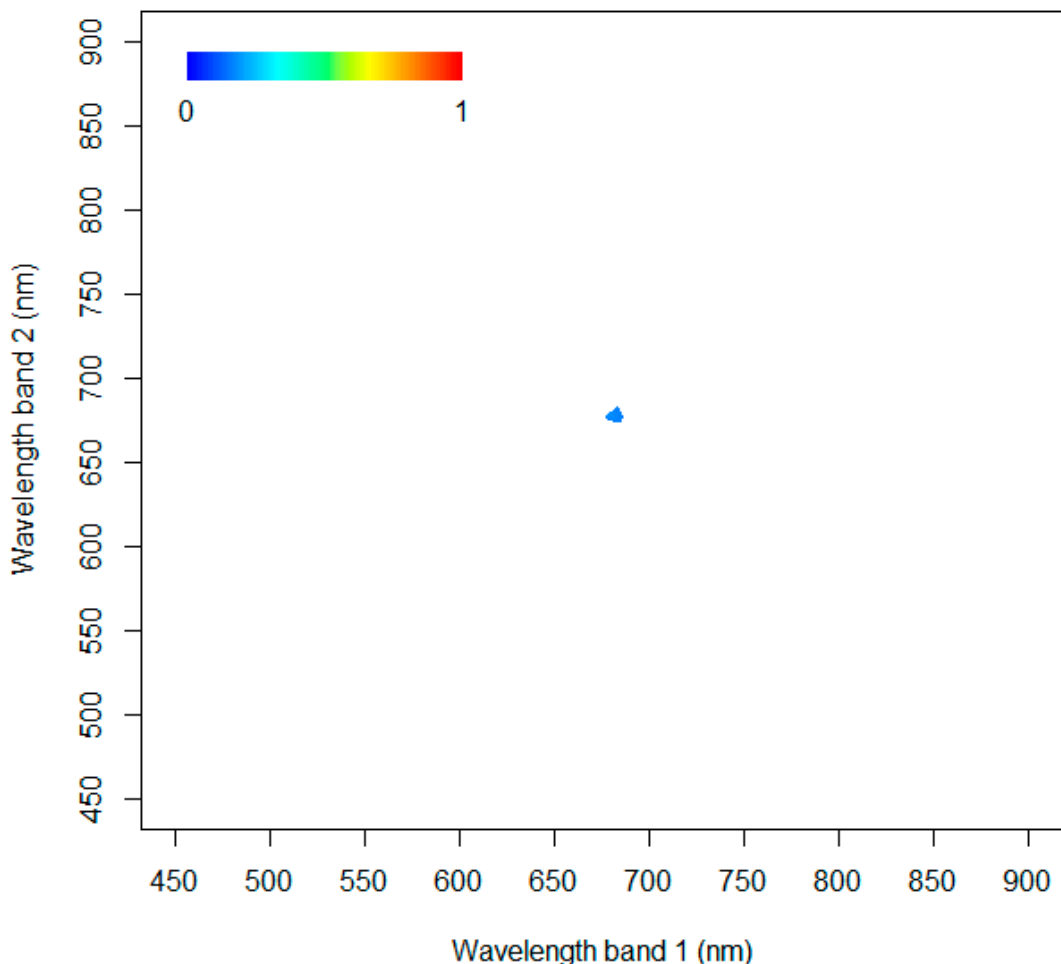
8

9      **Figure S1.** 2-D correlation plot illustrating the coefficient of determination ( $R^2$ ) of the  
10     normalised difference indices for all possible band combinations between 450 – 900 nm at  
11     hyperspectral resolution, for cyanobacteria artificially inoculated. Only the significant values ( $P$   
12     < 0.05) are represented.

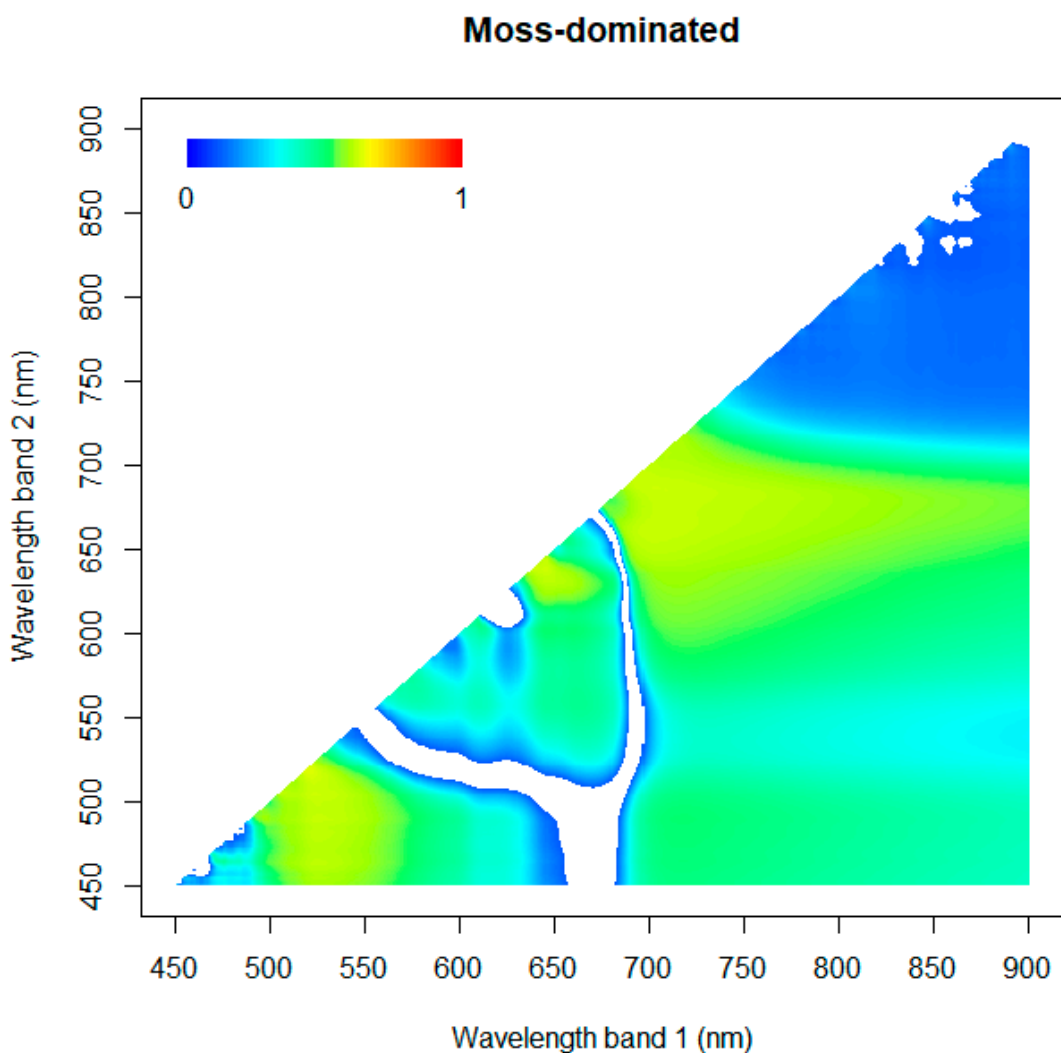


13  
14 **Figure S2.** 2-D correlation plot illustrating the coefficient of determination ( $R^2$ ) of the normalised  
15 difference indices for all possible band combinations between 450 – 900 nm at hyperspectral resolution, for  
16 natural cyanobacteria-dominated subsamples. Only the significant values ( $P < 0.05$ ) are represented.

### Lichen-dominated

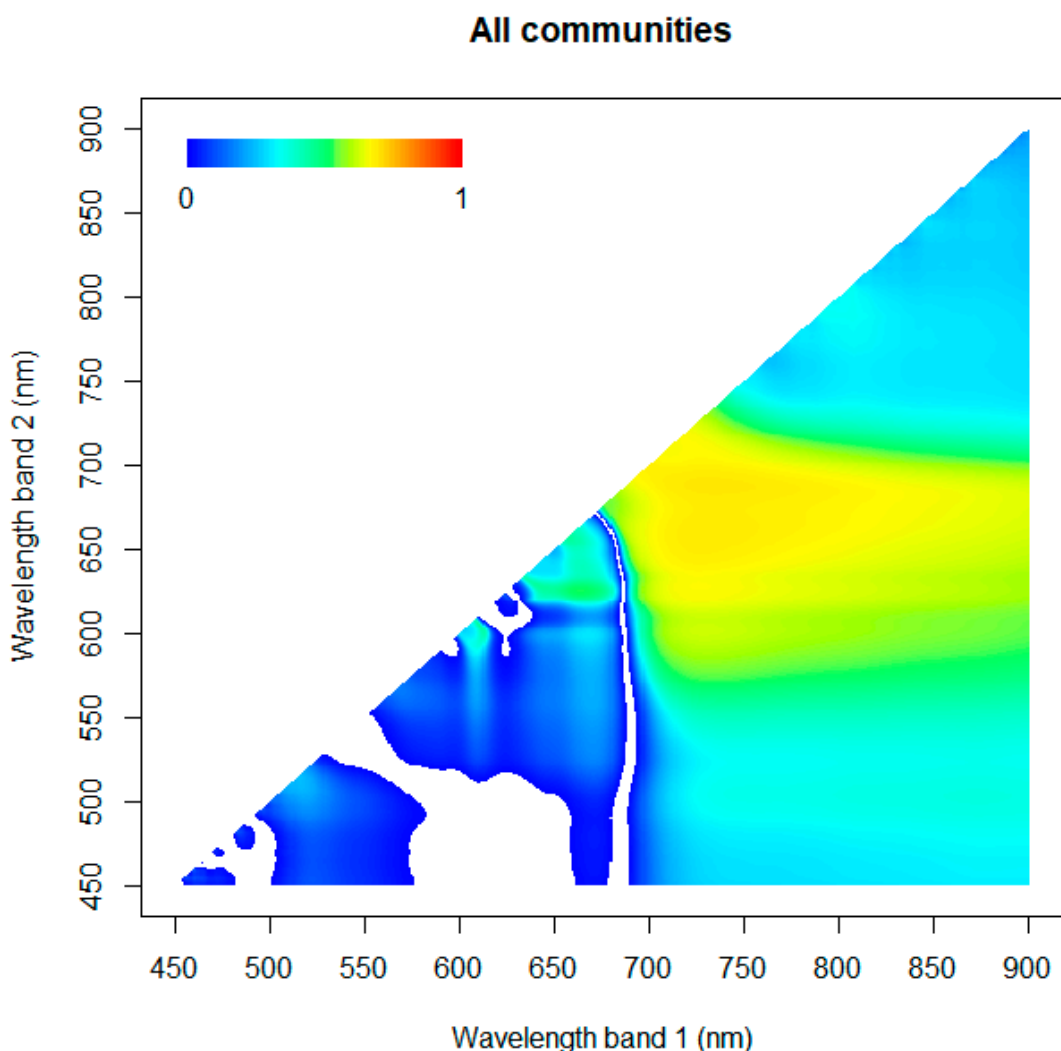


17  
18 **Figure S3.** 2-D correlation plot illustrating the coefficient of determination ( $R^2$ ) of the normalised  
19 difference indices for all possible band combinations between 450 – 900 nm at hyperspectral resolution, for  
20 natural lichen-dominated subsamples. Only the significant values ( $P < 0.05$ ) are represented.

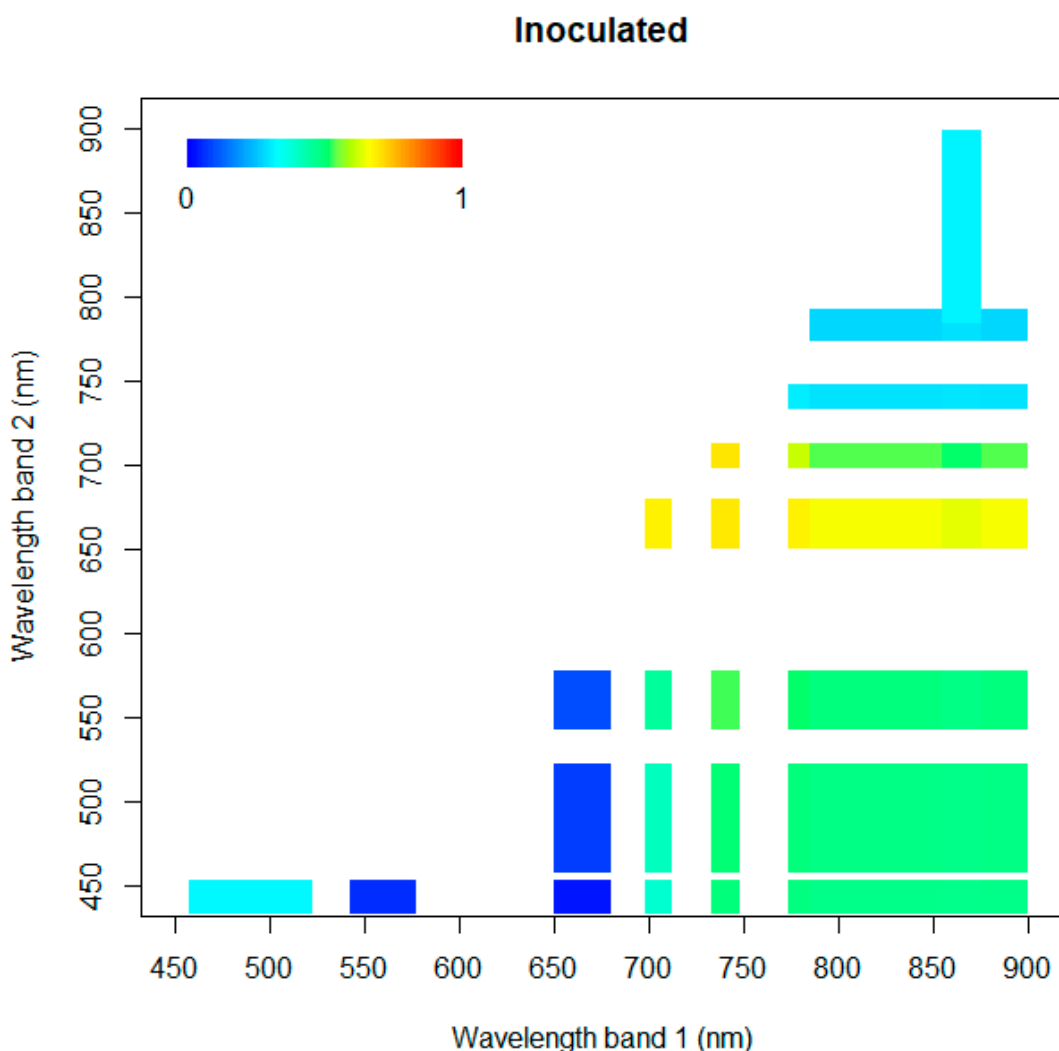


21

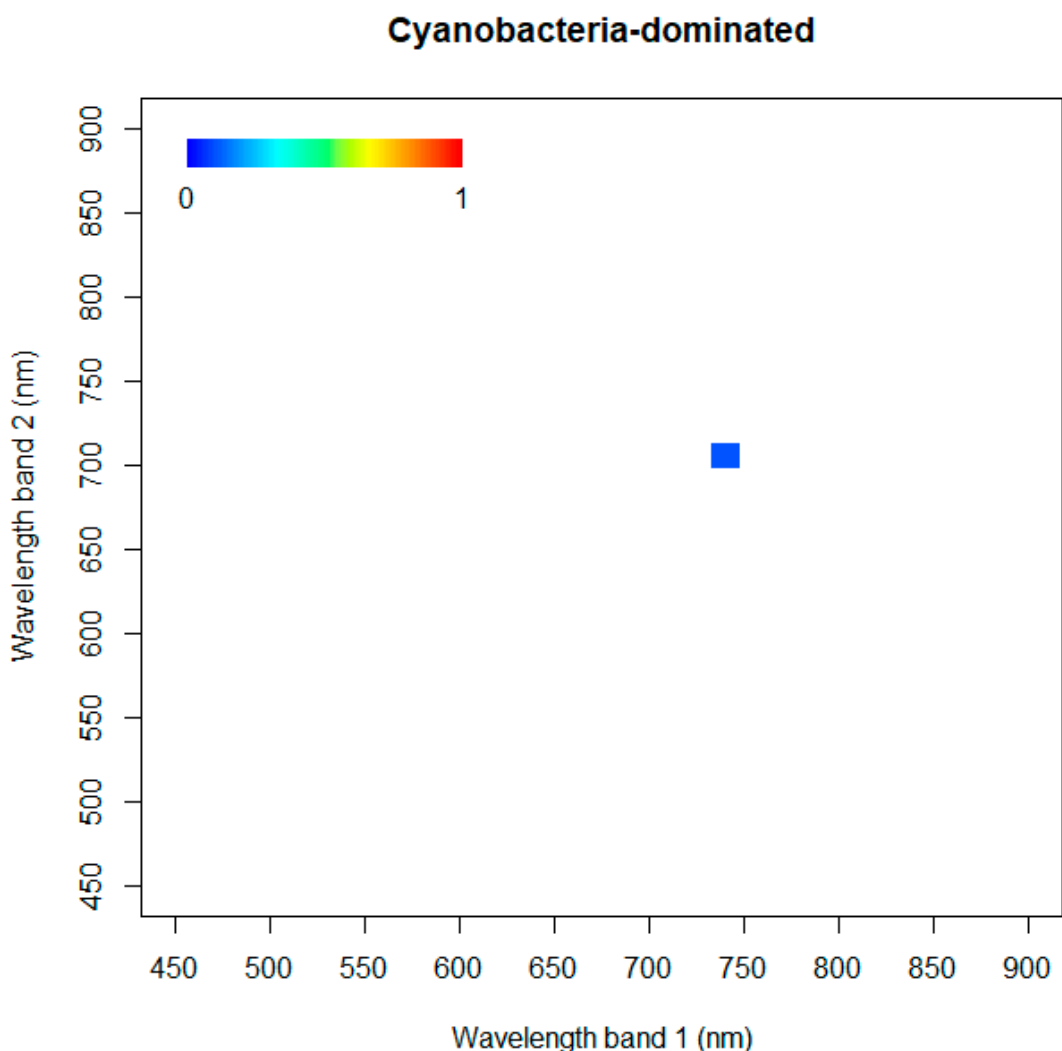
22 **Figure S4.** 2-D correlation plot illustrating the coefficient of determination ( $R^2$ ) of the normalised  
23 difference indices for all possible band combinations between 450 – 900 nm at hyperspectral resolution, for  
24 moss-dominated subsamples. Only the significant values ( $P < 0.05$ ) are represented.



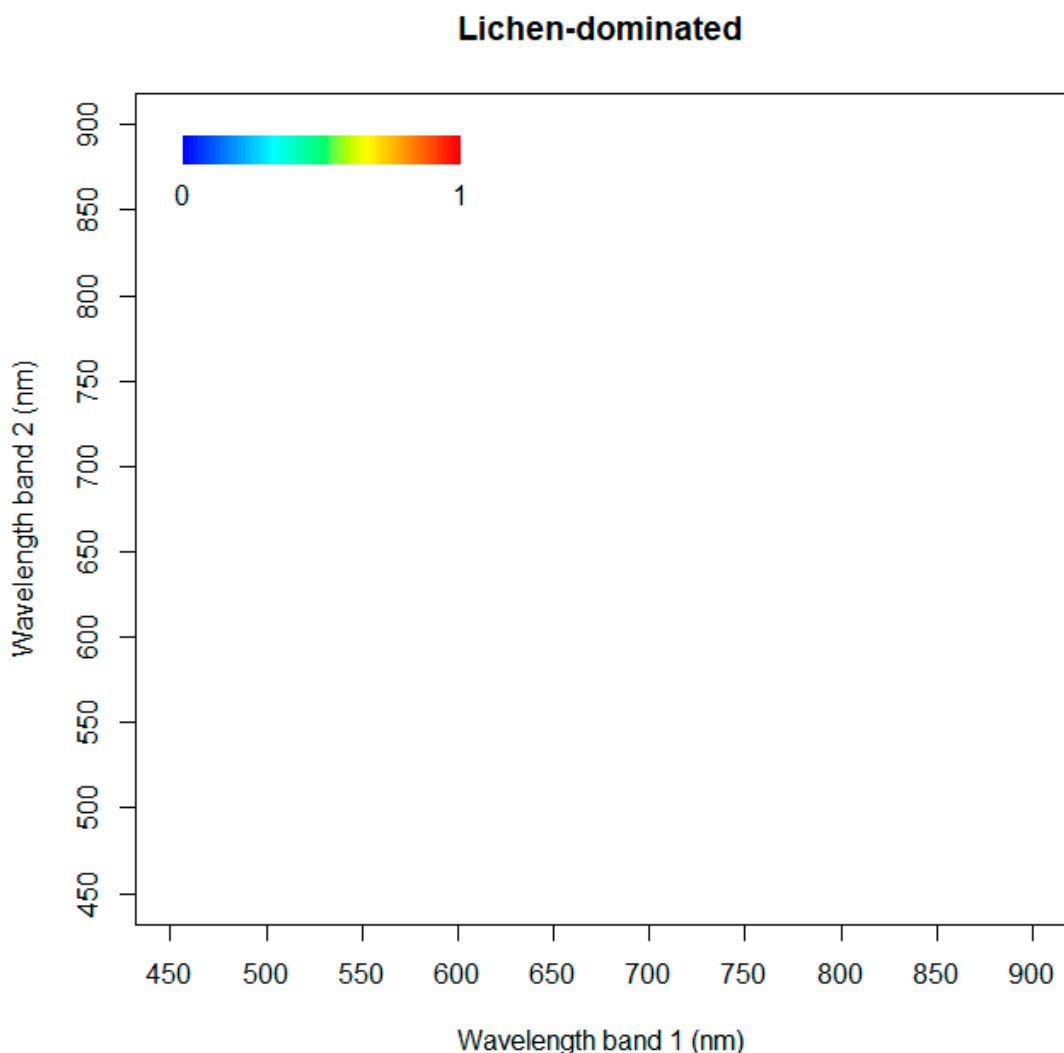
25  
26 **Figure S5.** 2-D correlation plot illustrating the coefficient of determination ( $R^2$ ) of the normalised  
27 difference indices for all possible band combinations between 450 – 900 nm at hyperspectral resolution, for  
28 the entire dataset. Only the significant values ( $P < 0.05$ ) are represented.



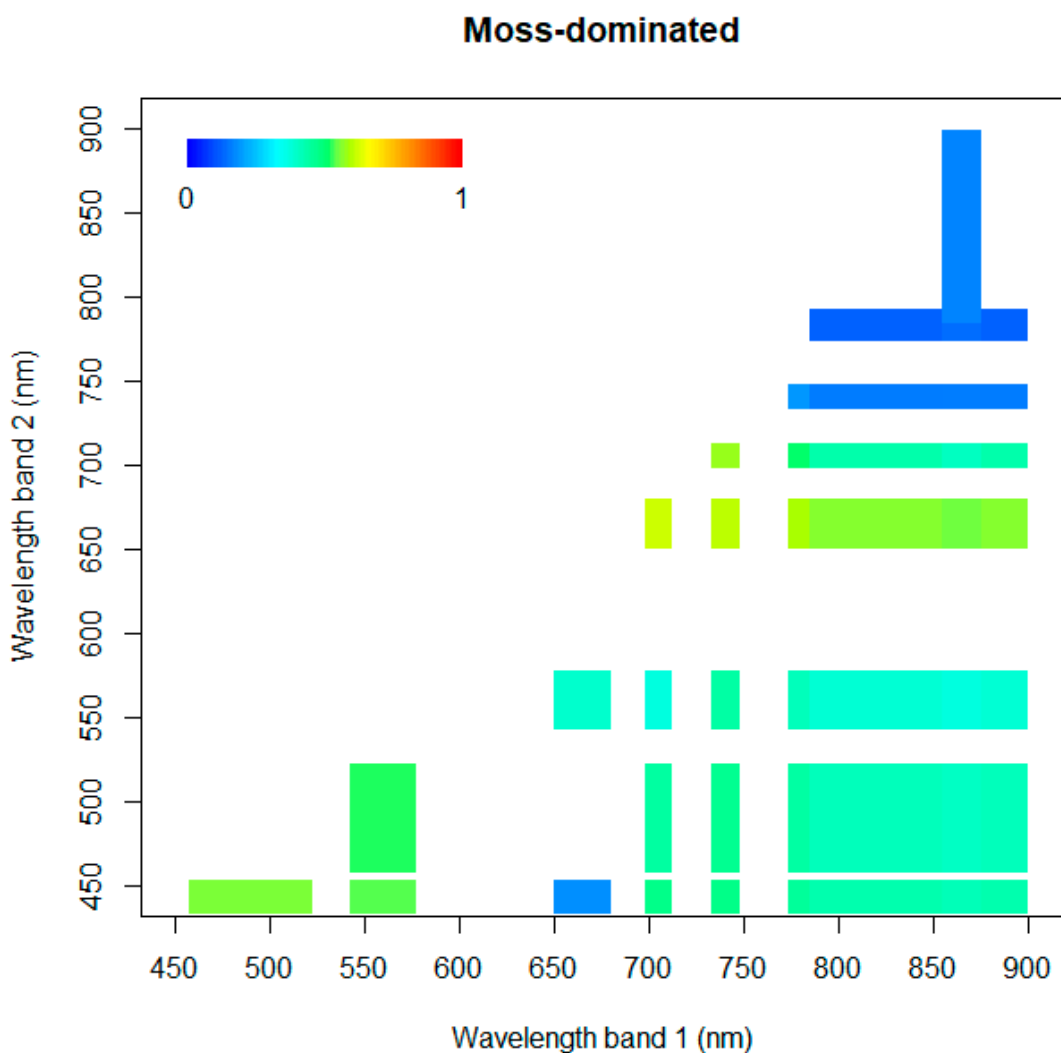
29  
 30 **Figure S6.** 2-D correlation plot illustrating the coefficient of determination ( $R^2$ ) of the normalised  
 31 difference indices for all possible band combinations between 450 – 900 nm at Sentinel-2 spectral  
 32 resolution, for artificially inoculated cyanobacteria subsamples. Only the significant values are represented  
 33 ( $P < 0.05$ ).



34  
35 **Figure S7.** 2-D correlation plot illustrating the coefficient of determination ( $R^2$ ) of the normalised  
36 difference indices for all possible band combinations between 450 – 900 nm at Sentinel-2 spectral  
37 resolution, for natural cyanobacteria-dominated subsamples. Only the significant values ( $P < 0.05$ ) are  
38 represented.



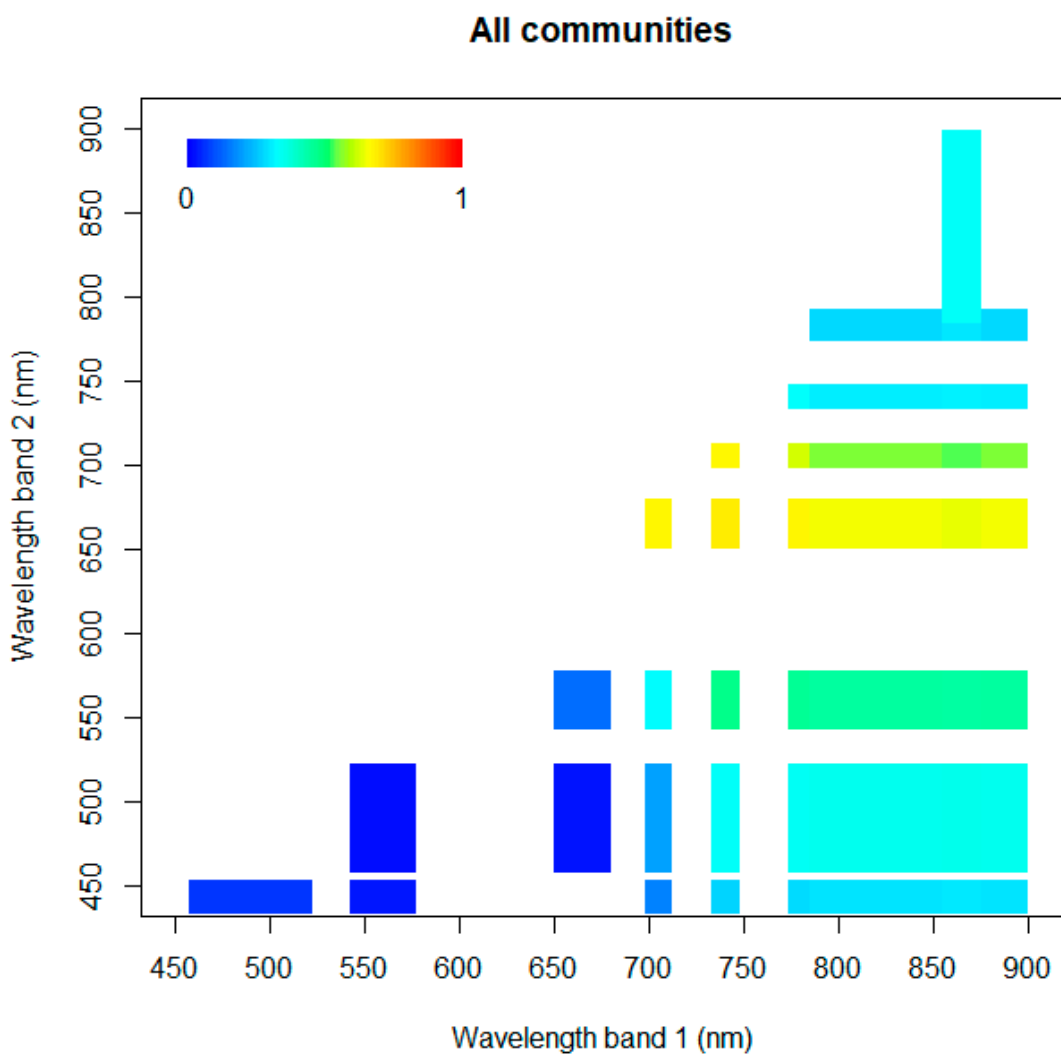
39  
40 **Figure S8.** 2-D correlation plot illustrating the coefficient of determination ( $R^2$ ) of the normalised  
41 difference indices for all possible band combinations between 450 – 900 nm at Sentinel-2 spectral  
42 resolution, for lichen-dominated subsamples. Only the significant values ( $P < 0.05$ ) are represented.



43

44 **Figure S9.** 2-D correlation plot illustrating the coefficient of determination ( $R^2$ ) of the normalised  
 45 difference indices for all possible band combinations between 450 – 900 nm at Sentinel-2 spectral  
 46 resolution, for moss-dominated subsamples. Only the significant values ( $P < 0.05$ ) are represented.

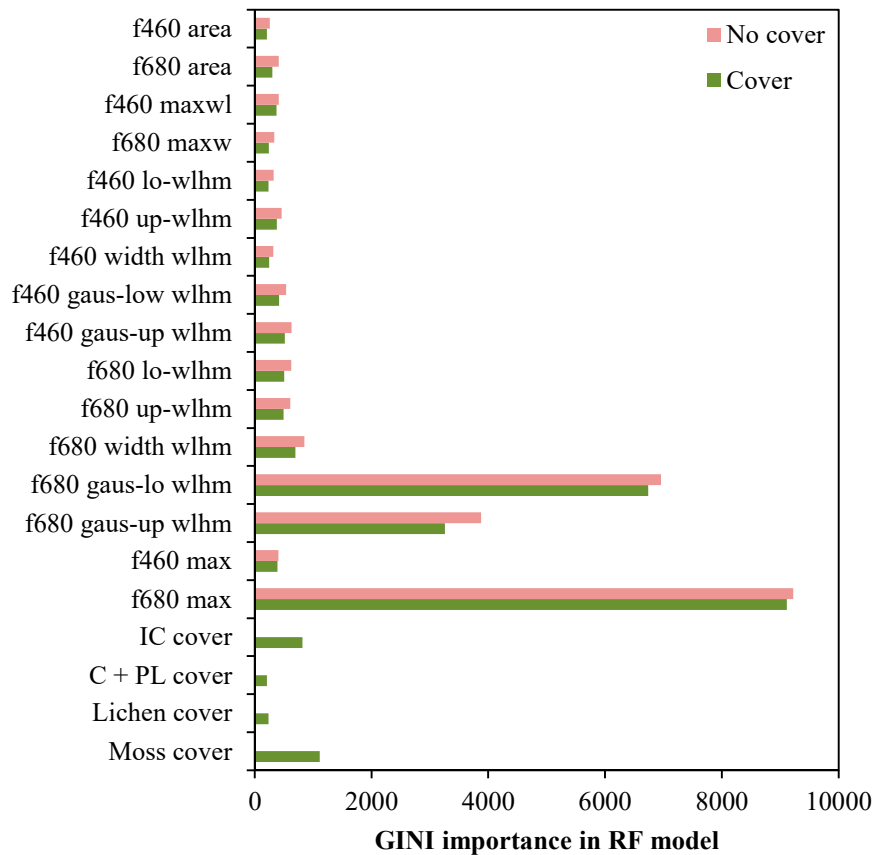
47



48

49 **Figure S10.** 2-D correlation plot illustrating the coefficient of determination ( $R^2$ ) of the normalised  
 50 difference indices for all possible band combinations between 450 – 900 nm at Sentinel-2 spectral  
 51 resolution for the entire dataset. Only significant values ( $P < 0.05$ ) are represented.

52



55      **Figure S11.** GINI importance of each variable in Random Forest model. Two options were tested: a) with  
 56      cover (green bars) and, b) without cover (pink bars). IC: Incipient cyanobacteria, C + PL: mix of  
 57      cyanobacteria and pioneer lichens.

60      **Supplementary references**

- 61      Chen, J.M., 1996. Evaluation of vegetation indices and a modified simple ratio for  
62      boreal applications. *Can. J. Remote Sens.* 22, 229–242.  
63      <https://doi.org/10.1080/07038992.1996.10855178>
- 64      Chen, J., Ming, Y.Z., Wang, L., Shimazaki, H., Tamura, M., 2005. A new index for  
65      mapping lichen-dominated biological soil crusts in desert areas. *Remote Sens. Environ.* 96, 165–175. <https://doi.org/10.1016/j.rse.2005.02.011>
- 67      Datt, B., 1998. Remote sensing of chlorophyll a, chlorophyll b, chlorophyll a+b, and  
68      total carotenoid content in eucalyptus leaves. *Remote Sens. Environ.* 66, 111–121.  
69      [https://doi.org/10.1016/S0034-4257\(98\)00046-7](https://doi.org/10.1016/S0034-4257(98)00046-7)
- 70      Daughtry, C.S.T., Walthall, C.L., Kim, M.S., De Colstoun, E.B., McMurtrey, J.E., 2000.  
71      Estimating corn leaf chlorophyll concentration from leaf and canopy reflectance.  
72      *Remote Sens. Environ.* 74, 229–239. [https://doi.org/10.1016/S0034-4257\(00\)00113-9](https://doi.org/10.1016/S0034-4257(00)00113-9)
- 73      Filella, I., Peñuelas, J., 1994. The red edge position and shape as indicators of plant  
74      chlorophyll content, biomass and hydric status. *Int. J. Remote Sens.* 15, 1459–1470.  
75      <https://doi.org/10.1080/01431169408954177>
- 76      Garrity, S.R., Eitel, J.U.H., Vierling, L.A., 2011. Disentangling the relationships between  
77      plant pigments and the photochemical reflectance index reveals a new approach  
78      for remote estimation of carotenoid content. *Remote Sens. Environ.* 115, 628–635.  
79      <https://doi.org/10.1016/j.rse.2010.10.007>
- 80      Huete, A.R., 1988. A soil-adjusted vegetation index (SAVI). *Remote Sens. Environ.* 25,  
81      295–309. [https://doi.org/10.1016/0034-4257\(88\)90106-X](https://doi.org/10.1016/0034-4257(88)90106-X)
- 82      Huete, A., Didan, K., Miura, T., Rodriguez, E.P., Gao, X., Ferreira, L.G., 2002. Overview  
83      of the radiometric and biophysical performance of the MODIS vegetation indices.  
84      *Remote Sens. Environ.* 83, 195–213.
- 85      Jordan, C.F., 1969. Derivation of Leaf-Area Index from Quality of Light on the Forest  
86      Floor. *Ecology* 50, 663–666. <https://doi.org/10.2307/1936256>
- 87      Karnieli, A., 1997. Development and implementation of spectral crust index over dune  
88      sands. *Int. J. Remote Sens.* 18, 1207–1220. <https://doi.org/10.1080/014311697218368>
- 89      Kochubey, S.M., Kazantsev, T.A., 2007. Changes in the first derivatives of leaf  
90      reflectance spectra of various plants induced by variations of chlorophyll content.  
91      *J. Plant Physiol.* 164, 1648–1655. <https://doi.org/10.1016/j.jplph.2006.11.007>
- 92      Le Maire, G., François, C., Dufrêne, E., 2004. Towards universal broad leaf chlorophyll  
93      indices using PROSPECT simulated database and hyperspectral reflectance

- 94 measurements. *Remote Sens. Environ.* 89, 1–28.  
95 <https://doi.org/10.1016/j.rse.2003.09.004>
- 96 Merzlyak, M.N., Gitelson, A.A., Chivkunova, O.B., Rakitin, V.Y., 1999. Non-destructive  
97 optical detection of pigment changes during leaf senescence and fruit ripening.  
98 *Physiol. Plant.* 106, 135–141. <https://doi.org/10.1034/j.1399-3054.1999.106119.x>
- 99 Penuelas, J., Filella, I., Baret, F., 1995. Semi-empirical indices to assess  
100 carotenoids/chlorophyll a ratio from leaf spectral reflectance. *Photosynthetica* 31,  
101 221–230.
- 102 Peñuelas, J., Gamon, J.A., Fredeen, A.L., Merino, J., Field, C.B., 1994. Reflectance  
103 indices associated with physiological changes in nitrogen- and water-limited  
104 sunflower leaves. *Remote Sens. Environ.* 48, 135–146. [https://doi.org/10.1016/0034-4257\(94\)90136-8](https://doi.org/10.1016/0034-4257(94)90136-8)
- 106 Román, J.R., Roncero-Ramos, B., Chamizo, S. Rodríguez-Caballero, E. Cantón, Y., 2018.  
107 Restoring soil functions by means of cyanobacteria inoculation: Importance of soil  
108 conditions and species selection. *L. Degrad. Dev.* 29, 3184–3193.
- 109 Rondeaux, G., Steven, M., Baret, F., 1996. Optimization of soil-adjusted vegetation  
110 indices. *Remote Sens. Environ.* 55, 95–107. [https://doi.org/10.1016/0034-4257\(95\)00186-7](https://doi.org/10.1016/0034-4257(95)00186-7)
- 112 Rouse, J.W., Haas, R.H., Schell, J.A., Deering, D.W., Harlan, J.C., 1974. Monitoring the  
113 vernal advancements and retrogradation of natural vegetation. In: NASA/GSFC,  
114 Final Report, Greenbelt, MD, USA, 1–137.
- 115 Schlemmer, M.R., Francis, D.D., Shanahan, J.F., Schepers, J.S., 2005. Remotely  
116 measuring chlorophyll content in corn leaves with differing nitrogen levels and  
117 relative water content. *Agron. J.* 97, 106–112.  
118 <https://doi.org/10.2134/agronj2005.0106>
- 119 Sims, D.A., Gamon, J.A., 2002. Relationships between leaf pigment content and spectral  
120 reflectance across a wide range of species, leaf structures and developmental  
121 stages. *Remote Sens. Environ.* 81, 337–354. [https://doi.org/10.1016/S0034-4257\(02\)00010-X](https://doi.org/10.1016/S0034-4257(02)00010-X)
- 123 Vogelmann, J.E., Rock, B.N., Moss, D.M., 1993. Red edge spectral measurements from  
124 sugar maple leaves. *Int. J. Remote Sens.* 14, 1563–1575.  
125 <https://doi.org/10.1080/01431169308953986>
- 126 Wu, C., Niu, Z., Tang, Q., Huang, W., 2008. Estimating chlorophyll content from  
127 hyperspectral vegetation indices: Modeling and validation. *Agric. For. Meteorol.*  
128 148, 1230–1241. <https://doi.org/10.1016/j.agrformet.2008.03.005>

129 Xue, L., Yang, L., 2009. Deriving leaf chlorophyll content of green-leafy vegetables from  
130 hyperspectral reflectance. ISPRS J. Photogramm. Remote Sens. 64, 97–106.  
131 <https://doi.org/10.1016/j.isprsjprs.2008.06.002>

132 Yoder, B.J., Pettigrew-Crosby, R.E., 1995. Predicting nitrogen and chlorophyll content  
133 and concentrations from reflectance spectra (400-2500 nm) at leaf and canopy  
134 scales. Remote Sens. Environ. 53, 199–211. [https://doi.org/10.1016/0034-4257\(95\)00135-N](https://doi.org/10.1016/0034-4257(95)00135-N)

136 Zarco-Tejada, P.J., Miller, J.R., Mohammed, G.H., Noland, T.L., Sampson, P.H., 2002.  
137 Vegetation Stress Detection through Chlorophyll + Estimation and Fluorescence  
138 Effects on Hyperspectral Imagery. J. Environ. Qual. 31, 1433.  
139 <https://doi.org/10.2134/jeq2002.1433>

140 Zhang, J., Huang, W., Zhou, Q., 2014. Reflectance variation within the in-chlorophyll  
141 centre waveband for robust retrieval of leaf chlorophyll content. PLoS One 9.  
142 <https://doi.org/10.1371/journal.pone.0110812>

143